RIVER RESEARCH AND APPLICATIONS

River. Res. Applic. **26**: 439–455 (2010)

Published online 16 July 2009 in Wiley InterScience
(www.interscience.wiley.com) DOI: 10.1002/rra.1281

THE RELATIONS BETWEEN 'STANDARD' FLUVIAL HABITAT VARIABLES AND TURBULENT FLOW AT MULTIPLE SCALES IN MORPHOLOGICAL UNITS OF A GRAVEL-BED RIVER

M. L. ROY,[a]* A. G. ROY[a] and P. LEGENDRE[b]

[a] *Département de Géographie, Université de Montréal, C.P.6128, Montréal, Qc, H3C 3J7, Canada*
[b] *Département de Sciences biologiques, Université de Montréal, C.P.6128, Montréal, Qc, H3C 3J7, Canada*

ABSTRACT

Fluvial fish habitat is often characterized by highly turbulent flow conditions. Several laboratory experiments suggest that unpredictable turbulent fluctuations can increase the swimming energy costs of fish. At the scale of fish habitat models, it can be hypothesized that turbulence can be captured by the combined effects of the standard habitat variables: depth, velocity and substrate. However, recent studies conducted at the reach scale suggest that turbulent properties are more controlled by the large-scale bed morphology than by individual roughness elements. In this study, we investigate the spatial structure of turbulent flow and the potential relationships between 'standard' habitat variables and turbulent flow properties in pools and riffles of a shallow gravel-bed river. The study explores these relations at multiple spatial scales. Mean turbulent properties and turbulent flow structures statistics were computed from 1932 near bed velocity time series sampled with acoustic Doppler velocimeters on a regular grid in four morphological units (two pools and two riffles) presenting a gradient of complexity. We used a novel multivariate variation partitioning analysis involving principal coordinates of neighbour matrices (PCNM) to partition turbulent flow properties into six significant spatial scales (VF: 0.35, F: 0.75, M: 1.25, L: 2, XL: 2.5 and XXL: 3 m). Between 45 and 70% of the variance of the turbulent flow properties were explained by the spatial PCNM. In the four units, turbulent properties exhibited a spatial dependence across the entire range of scales. However, the proportion of variation explained by the larger-scaled PCNMs was higher in the most homogeneous units. In general, the spatial dependence of turbulent flow was lower in the riffles than in the pools, where the mean flow velocity was slower. The capacity of 'standard' fish habitat variables to explain turbulent properties was relatively low, especially in the smaller scales, but varied greatly between the units. From a practical point of view, this level of complexity suggests that turbulence should be considered as a 'distinct' ecological variable within the range of spatial scales included in this study. Further research should attempt to link the spatial scales of turbulent flow variability to benthic organism patchiness and fish habitat use. Copyright © 2009 John Wiley & Sons, Ltd.

KEY WORDS: turbulence; fish habitat; PCNM; spatial modelling; ecohydraulics

Received 3 October 2008; Revised 10 April 2009; Accepted 6 May 2009

INTRODUCTION

Understanding the linkages between organisms and their hydraulic environment is a critical step in developing predictive models regarding the structure of fluvial ecosystems (Hart and Finelli, 1999). The temporal and spatial scales of flow variability are among the main drivers of numerous fluvial ecological processes (Biggs *et al*., 2005). One of the important issues in ecohydraulics research is to identify and match the proper fluvial scale to the ecological process or organism distribution of interest. At the smaller end of the spatio-temporal range of scales (millimetre to tens of metre, milliseconds to minutes), turbulent fluctuations can have direct and indirect effects on stream biota (Church, 2006). Three-dimensional rapid and often extreme velocity fluctuations occur around the time-averaged velocity across multiple scales (Hart *et al*., 1996). In gravel-bed rivers, velocity fluctuations are organized into coherent turbulent flow structures occupying the entire water column (Buffin-Belanger *et al*., 2000). Turbulence has an effect on the physical processes near the bed and on the forces applied to the particles composing

*Correspondence to: M. L. Roy, Département de Géographie, Université de Montréal, C.P.6128, Montréal, Qc, H3C 3J7, Canada.
E-mail: mathieu.roy.4@umontreal.ca

the substrate. Therefore, these forces play a role in sediment transport and bed morphology (Best, 1993). Turbulence also affects directly or indirectly numerous ecological processes such as resource distribution (Frechette *et al*., 1989), nutrient absorption by periphyton (Labiod *et al*., 2007), predator-prey interactions (Weissburg and Zimmerfaust, 1993) and agglomeration and destruction of algae (Stoecker *et al*., 2006). It also provides hydraulic habitat diversity, which could increase the abundance of ecological niches. Recent studies have also revealed that turbulence could affect fish swimming energy costs (Enders *et al*., 2003; Liao *et al*., 2003), habitat selection (Cotel *et al*., 2006; Smith *et al*., 2005; Smith *et al*., 2006) and capture efficiency (Enders *et al*., 2005). Turbulence can also provide a refuge from predator when water surface is skimming, affects water temperature and turbidity spatial distribution by means of mixing and could be responsible for the patchy distribution of benthic organisms (Quinn *et al*., 1996).

The effect of turbulence on the habitat selection of mobile organisms is complex as it may change as a function of scale and life functions (feeding, resting, reproduction, etc.). Moreover, the effect of turbulence at different scales could be conflicting. For example, a large-scale mixing layer could provide a positive abundance of nutrient whereas small scale intense fluctuations could cause a dislodgment of the organism. Furthermore, the effect may change with the type of physical habitat. For example, Liao *et al*. (2003) showed that fish were able to change their manner of swimming in the presence of artificially created periodic vortices in order to decrease their muscle activity. The fish could then use the energy from the vortices. In contrast, in more natural and unpredictable flows, fish exposed to higher levels of turbulence presented higher swimming energy expenditures (Enders *et al*., 2003). These results suggest that the 'type' of turbulence might influence fish energetics differently and may therefore affect habitat selection (Liao, 2007). However, the question of the effect of turbulence on fish habitat use in rivers remains to be explored.

Among the main challenges facing researchers investigating the effect of turbulence on ecological processes is the difficulty to isolate the effect of turbulence from the effect of other intercorrelated variables such as standard habitat variables commonly used in fish habitat models (mean flow velocity (U), depth (Y) and substrate size (D)). That is caused by the complex relationships between the variables that may change as a function of the spatial scale (Moir and Pasternack, 2008). The spatial distribution of turbulent flow properties at the micro-habitat scale around a pebble cluster or boulder have been previously described in detail (Brayshaw *et al*., 1983; Buffin-Belanger and Roy, 1998; Tritico and Hotchkiss, 2005; Lacey *et al*., 2007). Downstream from a roughness element, shedding motions are present, which results in an increase in turbulence intensity (Buffin-Belanger and Roy, 1998). However, the effect of roughness elements on flow properties is local. At the scale of pools and riffles, spatial patterns of turbulence properties might be controlled by the gross morphology rather than by individual boulders or pebble clusters (Lamarre and Roy, 2005; Legleiter *et al*., 2007). Smith and Brannon (2007) investigated the effect of roughness elements (fish cover habitats) on mean turbulent flow properties in riffles and pools and they observed a significant difference between turbulent kinetic energy in pools presenting abundant cover (high roughness) and without cover (low roughness) for juvenile salmonids. In contrast, they found no significant difference in the riffles, suggesting morphological units influence the effect of roughness on flow properties. Furthermore, at this scale, water depth could have an important effect on turbulence. For instance, the length and width of large-scale turbulent flow structures tend to scale with water depth (Roy *et al*., 2004). Moreover, these structures account for at least 50% of the total turbulent kinetic energy (Liu *et al*., 2001). Mean flow velocity is often correlated with turbulent intensity and turbulent flow structure properties, as when mean flow velocity, the standard deviation of the fluctuations (RMS_U) tends to increase (Nikora, 2006).

Several authors have proposed that future work should attempt to add turbulence metrics to fish hydraulic habitat models (Enders *et al*., 2003; Smith *et al*., 2006; Smith and Brannon, 2007). However, as turbulent properties might be strongly correlated to 'standard' habitat variables (velocity, depth and substrate size), their addition to habitat models may predominantly contribute redundant information. Furthermore, with the tools currently available, a characterization of turbulence in the field is costly and time-consuming. Nevertheless, habitats often present similar mean flow velocity and very different levels of turbulence. In spite of the observed correlation between mean flow velocity and turbulence intensity, the portion of turbulence variability explained by mean flow velocity, depth and bed roughness is currently not well known, as the relationships between the variables might change as a function of the spatial scale. Only a few studies have focused on the spatial distribution of turbulent flow

DOI: 10.1002/rra

properties at the scale of pools and riffles. To this date, we still lack a detailed description in different morphological contexts.

The quantification of the spatial structure of ecological processes and habitat is a major issue in current ecological studies. The spatial structure of ecological processes or species distribution can be attributed to two different sources. The first source is the inherent nature of the ecological process itself through the interrelations between neighbouring locations or individuals that cause autocorrelation (Legendre, 1993). A second source of spatial structuring on ecological processes is the effect of environmental or habitat variables which also have their own spatial structure. Similarly, environmental variables can also be structured by other environmental variables and the relationships between the variables can change according to the spatial scale at which it is described. For example, a relationship between two variables can be negative at a fine scale but positive at a larger scale. The most common tool used to describe the spatial structure of habitat and to link it to ecological processes is the combination of trend surface analysis with variation partitioning (Legendre and Legendre, 1998). Although this technique has proved successful and is widely used, trend-surface analysis only allows the broad-scale spatial variation to be modelled and does not allow to discriminate between the scales as the different polynomials are intercorrelated (Borcard and Legendre, 2002).

Borcard and Legendre (2002) have developed a spatial modelling method that provides a way to identify all the relevant spatial scales present in a dataset: the principal component of neighbour matrices (PCNM). This statistical technique achieves a spectral decomposition of the spatial relationships among the sampling sites, creating variables that correspond to all the spatial scales that can be found. This technique is analogous to Fourrier analysis, but provides a broader range of signals and can be used with irregularly spaced data (Borcard and Legendre, 2002). PCNM is a flexible tool as opposed to autoregressive models or trend surface, as these spatial variables can easily be incorporated into regression or canonical analysis models (Dray *et al*., 2006). Although PCNM was designed to describe and explain the spatial structure of ecological data, it is applicable to several other domains. For instance, it has been used to partition the spatial variability of vertical turbulent flow field at the micro-scale around a pebble cluster in a gravel-bed river (Lacey *et al*., 2007).

In this study, we investigated the planimetric spatial structure of turbulent flow close to the bed obtained from 1932 velocity measurements sampled across a systematic sampling grid in different morphological units. First, PCNM and canonical analysis were used to characterize the spatial structure of turbulent flow within two pools and two riffles in a shallow gravel-bed river. Then, we examined the potential causal relationships between standard habitat variables and turbulent flow properties at multiple scales using variation partitioning.

MATERIALS AND METHODS

Study site

Data were collected at the end of the summer 2004 on a section of the Eaton North River, located in the Eastern townships, approximately 200 km East of Montréal, Québec, Canada. At base flow, the width of the river ranged from 10 to 20 m and maximum flow depth was 1.5 m. The hydraulic and morphological properties of two pools and two riffles were characterized and mapped in detail. The four units presented a variety of morphological characteristics. Riffles 1 and 2 were located in a straight portion of the river, upstream from Pools 1 and 2. Pool 1 was located in a meander bend whereas Pool 2, a constriction pool maintained by a bedrock outcrop, was located 150 m downstream. The semi-alluvial context of Pool 2 created a much steeper slope than in the other units (Table I). The units covered an area ranging from 20 to 32 m^2.

Table I. Morphometric characteristics of the morphological units and discharge at the time of flow velocity sampling

	Slope (%)	D_{50} (mm)	Area (m^2)	Discharge ($m^3 s^{-1}$)
Riffle 1	0.2	55	20	2.49
Riffle 2	0.3	30	28	2.31
Pool 1	0.5	28	32	1.20
Pool 2	3	35	28	2.05

D50: median size of B-axis (Wolman, 1954).

DOI: 10.1002/rra

Field measurements

In every morphological unit, micro-topography and three-dimensional velocity measurements were sampled and mapped in detail. Micro-topography was mapped using a robotic total station (Trimble 5600DR) by combining a systematic transect sampling to a characterization of individual roughness elements. We characterized each particle or cluster of particles that was protruding at a height of approximately 15 cm or higher above the mean bed level. The average sampling densities in the four morphological units ranged from 29 to 36 points m^{-2}. From the micro-topography surveys, digital elevation models (DEMs) were created using a triangular irregular network interpolation. The topography sampling and the riverbed DEM were carried out according to guidelines outlined by Lamarre (2006).

A pressure transducer was used to record water level fluctuations and discharge was repeatedly estimated from cross-section flow measurements throughout the summer. Discharge values were then derived from a stage-discharge curve. The water level did not decrease by more than 1 cm within any of the flow measurement sessions. However, the discharge ranged from 1.2 to 2.5 $m^3 s^{-1}$ among the flow measurement sessions (Table I). Pool 2 was sampled at a discharge clearly lower than the three other units.

The 3D instantaneous streamwise, lateral and vertical velocity fluctuations were recorded in each morphological unit using two acoustic Doppler velocimeters (ADV, Sontek®, San Diego). Each ADV was attached to a steel wading rod. In the stream, the ADVs were moved between measurements and levelled by two operators. Velocities were measured at 10 cm above the bed. This height was determined in consideration of the difficulty to quickly obtain good quality data closer to the bed and the large number of samples required in this study. Flow velocity was sampled every 25 cm on a systematic sampling grid (16 points m^{-2}). Metal rods and strings were used as markers to build the sampling grid. The sampling grid of each unit was oriented towards the main downstream direction of flow. The locations close to the bank where depth was lower than 20 cm were not characterized because of the ADV instrumentation limitations.

Velocity time series quality check

Instantaneous velocities were recorded at each location for 80 s at 25 Hz, resulting in 2000 measurements per time series, which is higher than the optimal record length recommended by Buffin-Belanger and Roy (2005) for similar experimental protocols. A total of 1932 velocity time series were recorded in the four units. Each time series was plotted and visually inspected for obvious anomalies. As suggested by Lane *et al*. (1998) and the manufacturer, series presenting a correlation signal lower than 70% were rejected from further analysis. Low correlation signals can be caused by insufficient seeding in the clear water and echo noise arising from the irregular riverbed (Lacey and Roy, 2007). Doppler noise is inherent to all Doppler-based backscatter system signals. It is typically present over all frequencies. The removal of Doppler noise at high frequencies prevents biases in the estimation of turbulent statistics (Lane *et al*., 1998). Spectral analysis was also used as a mean to detect noise in the data. The slope of the power spectra within the inertial subrange was compared to the Kolmogorov $-5/3$ law. The series that exhibited a flat slope were removed from further analysis. This process resulted in the rejection of one to two percent of the series. Similarly, spikes in the velocity times series associated with instantaneous low signal correlations were detected using a phase-space thresholding filter (Goring and Nikora, 2002). As spikes in the signals are extreme values, their presence can bias the estimation of turbulence statistics. To insure data quality, data were removed when more than 5% of the series was modified by the filter. Less than one percent of the series were removed. Then, the data were filtered with a third-order Butterworth filter where the half frequency was equal to $fD/2.93 = 4.1$. For further details on this data quality check procedure, see Lacey and Roy (2007).

Habitat variables

From the microtopography and flow velocity data, 22 variables were created: three habitat variables (Table II; variables 1–3) and 19 turbulent flow variables (variables 4–22). Mean flow velocity (U) was derived from the longitudinal component of ADV time series. Water depth (Y) was obtained by subtracting the water level from the bed elevation values. A bed roughness (k) index was computed by estimating the standard deviation of elevation values in a window of 65×65 cm centered on each velocity measurement. A characterization of bed roughness

DOI: 10.1002/rra

Table II. All variables of the study in three categories: spatial variables, standard habitat variables and turbulence variables

Variable	Description	Riffle 1		Riffle 2		Pool 1		Pool 2	
		Avg	Std	Avg	Std	Avg	Std	Avg	Std
Spatial									
(x,y) (m)	Geographic coordinates (x,y)								
PCNMs	Spatial Eigenvectors								
Habitat									
1-U ($cm\,s^{-1}$)	Mean streamwise velocity	77.16	8.39	64.07	16.01	27.47	10.36	22.84	13.03
2-Y (m)	Depth	0.44	0.03	0.38	0.03	0.37	0.07	0.64	0.12
3-k (m)	Roughness index	0.02	0.01	0.03	0.01	0.03	0.02	0.05	0.02
Turbulence									
4-RMS_U ($cm\,s^{-1}$)	Root mean square streamwise velocity	11.64	1.64	12.98	2.97	6.93	1.63	7.99	2.72
5-RMS_V ($m\,s^{-1}$)	Root mean square—lateral	8.56	0.99	9.94	2.09	5.72	1.33	7.71	2.36
6-RMS_W ($m\,s^{-1}$)	Root mean square—streamwise	5.93	0.82	7.23	1.63	3.72	1.19	5.30	1.72
7-τ ($N\,m^{-2}$)	Mean Reynolds shear stress	26.17	10.49	35.20	21.87	8.55	6.10	10.73	11.09
8-TKE ($cm^2\,s^{-2}$)	Turbulent kinetic energy	124.10	30.63	167.60	69.03	50.14	23.65	84.14	50.73
9-ITS_U (s)	Integrated time scale—streamwise	0.41	0.13	0.24	0.05	0.72	0.38	0.66	0.46
10-ITL_U (cm)	Integrated length scale—streamwise	31.94	11.10	15.07	4.52	18.58	9.66	12.31	7.23
11-ITS_V (s)	ITS—lateral	0.16	0.08	0.13	0.03	0.34	0.21	0.60	0.50
12-ITS_W (s)	ITS—vertical	0.13	0.02	0.12	0.02	0.32	0.23	0.38	0.27
13-ITL_W (cm)	ITL—vertical	9.90	1.69	7.39	1.62	7.17	2.79	6.48	2.91
14-Q1-p (%)	Proportion of time high speed outward	9.69	1.02	9.02	1.70	8.25	1.76	6.68	2.11
15-Q1-d (s)	Mean duration of events—$Q1$	0.11	0.01	0.10	0.01	0.13	0.04	0.14	0.04
16-Q4-p (%)	Mean propotion of time occupied by incursions	2.08	0.62	2.39	1.25	2.54	1.11	3.90	1.95
17-Q4-d (s)	Mean duration of events—$Q4$	0.07	0.01	0.07	0.01	0.08	0.02	0.11	0.04
19-HS-N	Frequency of HS events (U-level)	65.39	8.38	73.45	11.78	71.45	18.37	58.86	16.28
20-HS-P (%)	Proportion of time- high speed events (U-level)	10.40	0.71	10.00	0.80	9.66	0.96	9.43	1.16
21-HS-D (s)	Mean duration of HS events (U-Level)	0.13	0.02	0.11	0.02	0.12	0.04	0.14	0.04
22-HS-Max (s)	Maximum duration of HS events (U-level)	0.70	0.23	0.53	0.17	0.73	0.38	0.90	0.52

Velocity measurements were taken 10 cm above the bed. Spatial average and standard deviations are presented.

DOI: 10.1002/rra

based on bed elevation is less common in the ecological literature than the more traditional approach based on particle size distributions (e.g. Wolman, 1954). The latter makes the assumption that bed arrangement and particle shape, orientation, packing, spacing, sorting and clustering are homogeneous (Nikora *et al*., 1998). However, this assumption is not always appropriate. For example, it is common to observe large particles buried in the bed that do not protrude higher above the bed than smaller particles. In contrast, our index based on bed elevation provides a direct measure of bed roughness that might be more relevant in affecting flow properties and providing cover for fish.

From the velocity time series, several types of turbulence variables were created (Table II). Time averaged turbulent statistics were estimated at each measurement point. These included turbulent intensities, the root mean squared streamwise, lateral and vertical velocities (RMS_u, RMS_v, RMS_w), the mean Reynolds shear stress ($\tau = -\rho uv$), where ρ is the water density and uv the covariance of the streamwise and vertical velocity and the turbulent kinetic energy, a combination of the turbulent intensities in the three dimensions ($TKE = 0.5 (u'^2 + v'^2 + w'^2)$). Integral timescales (ITSu, ITSv and ITSw) were derived by integrating the autocorrelation functions of the streamwise, lateral and vertical velocity components over time.

$$\mathrm{ITS}_x = \int_{t=0}^{T=t} Rxx(\Delta t)\mathrm{d}t \tag{1}$$

ITSu, ITSv and ITSw therefore represent the length of time over which each velocity component presents a significant positive autocorrelation. This variable is sometimes referred to as *eddy length*. The integral length scale (*ITL*), obtained by multiplying the ITS by U, was used to estimate the spatial extent of the turbulent structures.

Turbulent properties were also estimated using two types of turbulent event detection techniques. First, we used quadrant analysis as described by Lu and Willmarth (1973) with a threshold value of $Th = 2$, which means that only the strong events remained in the analysis (Table II variables 14–17). The proportion of time (p) and the duration (d) of the events were estimated for quadrant 1 ($Q1$) and 4 ($Q4$). *Q1* and $Q4$ are associated with the streamwise high-speed events. The events in $Q4$ are related to the occurrence of sweep structures known to be accountable for shear stress generation whereas $Q1$ is related to high speed outward interactions (Buffin-Belanger and Roy, 1998). Second, we used the modified U-level technique to detect the occurrence of macroturbulent flow structures (Luchik and Tiederman, 1987). This method tracks changes in the longitudinal velocity components as follows. The beginning of a turbulent event begins when $|u'| > ks_u$ and ends when $|u'| < \mathrm{pks}_u$, where u' is a velocity fluctuation around the average, k is a threshold and s_u is the standard deviation of the velocity fluctuations and p takes a value between 0 and 1. Here, a threshold of $k = 2$ and $p = 0.25$ was used. In the present study, the variables associated with low-speed, $Q2$ (ejections) and $Q3$ (inward interactions), were very strongly correlated to the high speed variables ($Q1$ with $Q3$ and $Q2$ with $Q4$) Therefore, we chose to focus on the high speed events rather than on the low-speed, as we suppose in many cases they may have a stronger impact on biota, such as dislodgement of organisms.

Turbulent flow variables were tested for normality (K-S test) and transformed when it was necessary using a Box–Cox (1964) normalization procedure. As all turbulence variables did not bear the same physical units, they were also centred and standardized.

Study sites

The four sites presented a wide range of hydraulic environments. Table II summarizes the statistics of the four units. Space averaged mean flow depth (Y) did not vary greatly between the units. However, the pools presented a higher standard deviation than riffles, which illustrates the wider range of depth values. Furthermore, mean bed roughness (k) was higher in the pools than in the riffles, Pool 2 presenting the roughest bed and Riffle 1 the smoothest. The average mean streamwise velocity (U) ranged from 21 to 62 $\mathrm{cm\,s^{-1}}$ and was two to three times higher in the riffles than in the pools (Figure 1, Table II). Similarly, the mean values of turbulent properties (RMS, τ and TKE) in the riffles were higher than in the pools. In general, the four units presented a gradient of hydraulic

DOI: 10.1002/rra

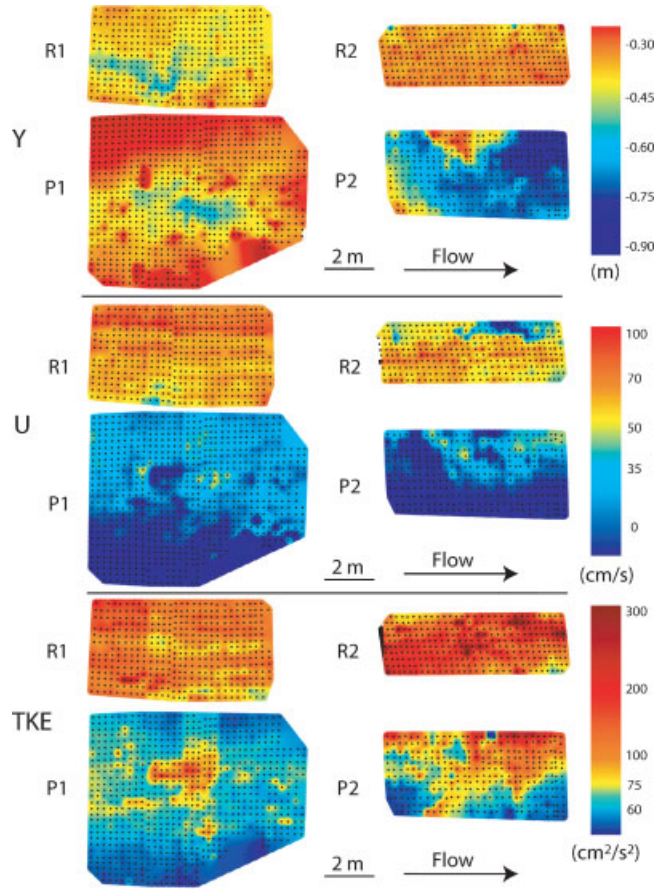

Figure 1. Colour plots of depth (Y), mean streamwise flow velocity (U) and turbulent kinetic energy (TKE) for the four morphohygraulic units Riffle 1 (R1), Riffle 2 (R2), Pool1 (P1) and Pool 2 (P2). Flow velocity was sampled every 25 cm on a regular sampling grid (points).

heterogeneity. The gradient from the most heterogeneous to the most homogeneous unit was Riffle 2, Riffle 1, Pool 1 and Pool 2.

Turbulent flow spatial scale partitioning: PCNM statistical analysis

The PCNM method developed by Borcard and Legendre (2002) allows the determination of the proportion of the variation of the response variables variation explained by spatial patterns at each spatial scale. Based on the spatial coordinates, the PCNM analysis creates a set of explanatory spatial variables (eigenvectors), further referred as *PCNMs*, which represent the range of spatial frequencies that can be perceived on the sampling grid, given the sampling design (Borcard *et al*., 2004). These distance-based eigenfunctions are orthogonal to one another and therefore do not present intercorrelations (Dray *et al*., 2006). The *PCNMs* are constructed through a series of operations presented in Figure 2. For regular sampling designs, *PCNMs* are sinusoidal and of decreasing periods. We grouped them into six spatial scales. The four morphological units were processed separately. The following will briefly describe the five steps involved in the PCNM analysis. In the sixth step, PCNM-turbulence model outputs will be linked to standard habitat variables. For further details on the method, see Borcard and Legendre (2002) and Borcard *et al*. (2004).

Step 1: Euclidian distance matrix

A pairwise Euclidian distance matrix was computed from all the geographic coordinates of each velocity measurement.

DOI: 10.1002/rra

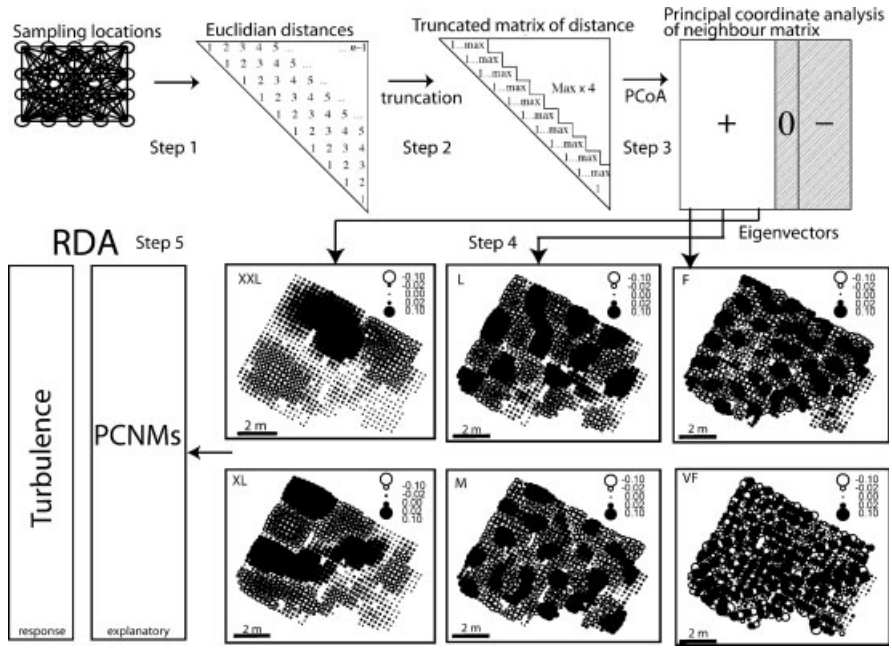

Figure 2. Schematic diagram of principal component of neighbour matrices (PCNM) methodology. Step 1: from the spatial coordinates, a matrix of the Euclidian links between the samples was built. Step 2: the distance matrix was truncated at a distance (0.25 m). Step 3: a matrix of eigenvectors was obtained by Principal coordinates analysis of the truncated matrix. Step 4: all positive eigenvectors (PCNMs) were mapped and grouped in spatial scales. The figure presents six examples of PCNMs constructed from the coordinates of Pool 2, selected from each of the spatial scales. XXL: 3–4 m, XL: 2.5–3 m, L: 1.5–2.5 m, M: 1–1.5 m, F: 0.5–1 m, VF: 0.25–0.5 m. The size of the circles is proportional to the magnitude of the *PCNMs* values. Step 5: each groups of *PCNMs* associated to a specific scale were used as explanatory variables in canonical analysis (RDA) to explain the variability of turbulent flow variables. Modified from Borcard *et al*. (2004)

Step2: truncation of the distance matrix

A threshold value (t) was chosen and used to build a truncated distance matrix as follows:

$$D^* = \left\{ \begin{array}{l} dij \text{ if } dj \leq t \\ 4t \text{ if } dj > t \end{array} \right\} \tag{2}$$

For all four morphological units, the threshold value was set to 0.25 m, a value corresponding to the sampling interval, as recommended for regular sampling design because it keeps all the sampling locations connected in a single network (Borcard *et al*., 2004).

Step 3 Generating PCNMs: Principal coordinate analysis (PCoA) on the truncated distance matrix

A set of eigenvectors was obtained by performing a principal coordinate analysis (PCoA) on the truncated distance matrix (D^*). PCoA, also known as 'classical scaling', is a common ecological ordination method based on linear scalings (Gower, 1966). The *PCNMs,* the positive eigenvectors, include all the spatial scales that can be analysed in each sampling grid. Eigenvectors associated with large eigenvalues contain the larger-scale variability whereas the lower eigenvalues represent the fine-scale variability. Because the distance matrix was truncated, a portion of the eigenvectors had negative eigenvalues. These were removed from the analysis. For each morphohydraulic unit, the number of positive eigenvectors was approximately equal to two-thirds of the number of samples (Borcard *et al*., 2004). Therefore, Pool 1 presented much more *PCNMs* than the other units. All PCNM analyses were carried out using the R language software (Comprehensive R Archive Network, http://cran.r-project.org/) and the spacemakerR package (Dray *et al*., 2006).

DOI: 10.1002/rra

Step 4: defining relevant spatial scales

A forward selection permutation method was used to determine which PCNMs were explaining a significant portion of the variability of the turbulent flow variables. Between 20 and 30% of the *PCNMs* per unit significantly explained turbulent flow variability and were therefore selected (Table III). For each spatial scale, the *PCNMs* were used as explanatory spatial variables to explain the variability of turbulent flow properties using canonical redundancy analysis (RDA). RDA is the direct extension of multiple regression to model multivariate datasets (Legendre and Legendre, 1998). All significant *PCNMs* were mapped on the geographic coordinates and visually inspected. Figure 2 illustrates examples of *PCNMs* maps for Pool 1. Selecting the number of PCNM submodels is a subjective process. We divided the spatial eigenfunctions in six submodels corresponding to spatial scales: very large +(XXL), very large –(XL), large (L), medium (M), fine (F) and very fine (VF). The physical scale associated to these arbitrary spatial scales was set by inspecting the half-periods of the *PCNMs* Table III. The minimum scale size is restricted by the sampling interval (0.25 m) and by the extent of the morphohydraulic units (4 m). In order to compare between the units, we set the maximum spatial scale to be the largest scale of the smallest unit. Any variability occurring beyond the range of scales was not taken into account by the analysis.

Step 5: spatial scale partitioning of turbulent flow properties: canonical redundancy analysis (RDA)

For each spatial scale, RDA was used to determine the proportion of variability of the 19 turbulence variables explained by the *PCNMs* associated to that specific scale. R^2 is an indicator of the importance of the contribution of *PCNMs* to the variation of turbulent flow variables. R^2 values were adjusted for the explanation that would be provided by the same number of random explanatory variables measured over the same number of objects (Ezekiel, 1930).

Step 6: the relationships between turbulence and standard habitat variables at all spatial scale: variation partitioning

In this step, the relationships between habitat variables (U, Y and k) and turbulent flow properties at each spatial scale was assessed with a variation partitioning procedure using the function 'varpart' of the Vegan R-language package (Oksanen *et al*., 2007). Habitat variables were used as explanatory variables to explain the variability of the first canonical axis of the RDAs previously obtained for each scale in step 5. In this process, habitat variables are run successively in multiple regression models as co-variables and subsequent variables need to explain a significant amount of the residual variance (Monte Carlo, 999 permutations). This procedure, automated in the 'varpart' function, allowed us to discriminate between the fractions of variation explained by a single habitat variable from the portion explained by two or three intercorrelated variables. Finally, multiple regression models were used to

Table III. Classification of PCNM variables (PCNMs)

	Scales		Morphohydraulic units			
		Physical (m)	Riffle 1	Riffle 2	Pool 1	Pool 2
Number of sig. PCNMs	+Extra large (XXL)	3.0–4.0	6	3	9	4
	Extra large (XL)	2.5–3.0	5	6	17	8
	Large (L)	1.5–2.5	12	7	27	12
	Medium (M)	1.0–1.5	11	13	29	17
	Fine (F)	0.5–1.0	11	18	34	25
	Very fine (VF)	0.25–0.5	9	19	36	22
	Total		54	66	152	94
	Total PCNMs		302	214	561	232
	Number of samples		432	307	800	343

Number of variables in each spatial scales. The physical scale ranges were subjectively defined based on the half periods of the PCNMs.

DOI: 10.1002/rra

investigate the spatial structure of single turbulence variables and to break down the variation into contributions from each spatial scale.

RESULTS

In each morphological unit, an important proportion of turbulent flow variability was explained by the spatial component of the data. The canonical redundancy analyses based on the *PCNMs* at each spatial scale explained a significant portion of variation of turbulent flow properties with adjusted coefficients of determination (R^2_a) ranging from 0.44 to 0.70 (Figure 3; Table IV). R^2_a values were higher for the pools than the riffles. Six successive RDA revealed the proportion of variation explained by each spatial scale. In general, turbulent flow variables showed a spatial structure across multiple scales at all four sites. The six spatial scales explained a minimum of 7% and a maximum of 42% percent of the total explained turbulent flow variability. In Riffle 1, the L scale (1.5–2.5 m) was dominant, with 34% of the variation explained. Similarly, the spatial structure in Pool 1 was dominated by one

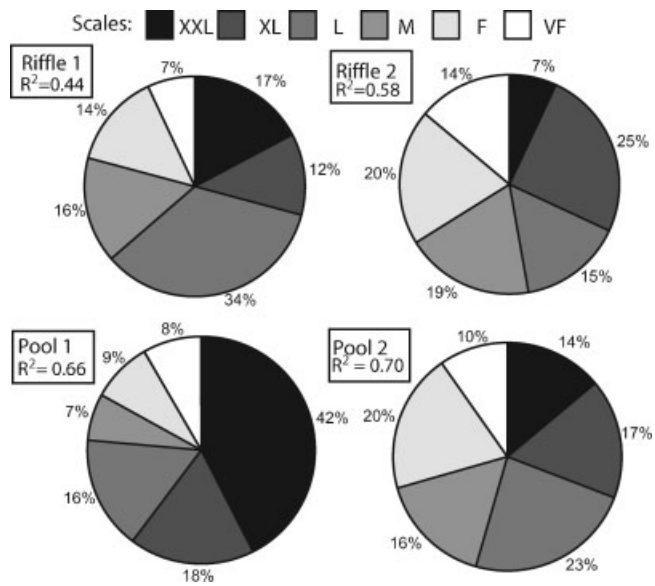

Figure 3. The values in rectangles express the total variation explained by all scales (R^2_a). Pie charts present the break down of explained variance per PCNM spatial model (XXL: 3–4 m, XL: 2.5–3 m, L: 1.5–2.5 m, M: 1–1.5 m, F: 0.5–1 m, VF: 0.25–0.5 m)

Table IV. Significant canonical Eigenvalues of the first (λ_1) and second axis (λ_2) and adjusted R^2 of the RDA expressing the proportion of turbulent flow properties explained by PCNMs at each spatial scale in each morphohydraulic unit ($p \leq 0.05$)

	Riffle 1			Riffle 2			Riffle 3			Riffle 4		
Scales	λ_1	λ_2	R^2	λ_1	λ_2	R^2	λ_1	λ_2	R^2	λ_1	λ_2	R^2
XXL	0.03	0.02	0.06	0.03	NS	0.04	0.13	0.09	0.27	0.05	0.04	0.10
XL	0.03	0.01	0.04	0.08	0.04	0.14	0.05	0.04	0.11	0.05	0.04	0.11
L	0.09	0.02	0.12	0.05	0.01	0.08	0.06	0.02	0.10	0.07	0.06	0.17
M	0.03	0.01	0.06	0.04	0.03	0.10	0.02	NS	0.04	0.05	0.03	0.11
F	0.03	0.01	0.05	0.05	0.02	0.11	0.02	NS	0.06	0.07	0.03	0.13
VF	0.01	0.01	0.02	0.03	0.02	0.08	0.03	NS	0.05	0.03	0.02	0.07

DOI: 10.1002/rra

spatial scale, with XXL *PCNMs* explaining most variability (42%). In contrast, the variability of turbulent flow in Riffle 2 and Pool 2 was divided more evenly across the spatial scales. These showed higher standard deviations of the turbulent variables indicating that they were more spatially heterogeneous than Riffle 1 and Pool 1, which were dominated by the large-scale patterns among the variables. The variability of turbulence explained by the F and VF scales was also higher for Pool 2 and Riffle 2. However, the variance explained in these scales always remained under 20% of the total.

Multiple regression models show that the behaviour of each variable presented a great variability between the sites (Figure 4). In general, the variables did not exhibit much difference between each other in the smaller scales (M, F, VF). The spatial structure observed in the larger scales (L, XL, XXL) was more important distinguishing the variables in Riffle 1, Riffle 2 and Pool 1. For instance, in Riffle 1, where spatial dependence was the lowest in general, the variables related to turbulence intensities (RMS_u, RMS_v, RMS_w and TKE) and the length and duration of turbulent flow structures (ITS and ITL) were the most spatially structured. In contrast, the turbulent structure variables (Q and HS) showed a low spatial dependence in the range of scales. The main difference between the variables was the contribution of the L-scale (1.5–2.5 m), which was more important for mean turbulent variables (RMS, τ, TKE) than for the turbulent event variables. A similar spatial structure was observed in Pool 1, except for one scale, the XXL scale (3–4 m), and in Riffle 2, where a strong spatial coherence in the XL scale (2.5–3 m) was observed. In contrast, Pool 2 showed very low variation in spatial structure between the turbulence variables and scales.

In each morphological unit, RMS and TKE were always among the most spatially structured variables and the spatial organisation of Reynolds shear stress was slightly less marked. Variables describing the turbulent flow events obtained from quadrant analysis generally presented the lowest spatial coherence, except in Pool 2. Similarly, the proportion of time and maximum duration of high-speed turbulent events (HS-*P*, HS-Max) presented the lowest R^2_a. In contrast, the duration and frequency of high speed events (HS-*d*, HS-*N*) presented a spatial structure across a range of scales: mainly larger scales in Pool 1, mainly finer scales in Riffle 2 and all scales in Pool 2.

The relationships of standard habitat variables with turbulent flow variables at each scale were investigated using a variation partitioning procedure. The fraction of variation explained by mean flow velocity, flow depth, bed roughness and the fraction shared by two or more variables are presented in Figure 5. The coefficients of determination are shown for significant canonical axis only. In all morphological units, the proportion of variation explained by standard habitat variables for the combined scales ranged from 0.25 to 0.65. It was considerably lower

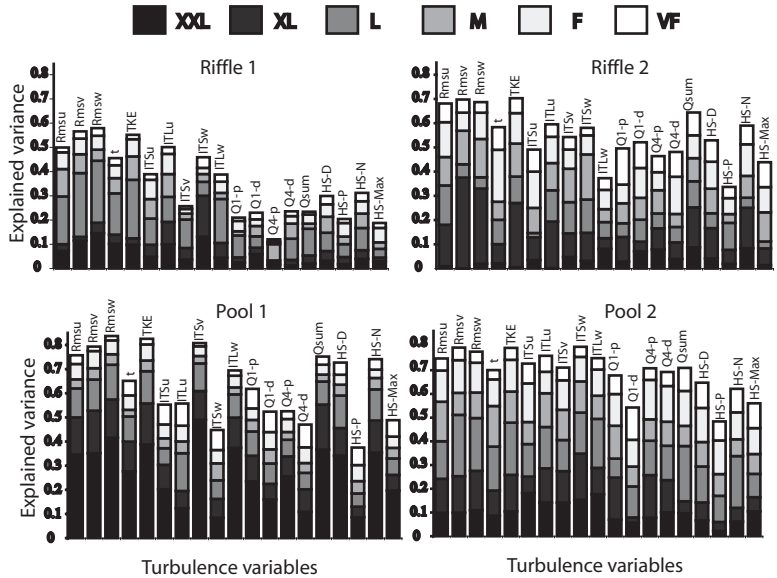

Figure 4. Fractions of explained variance (adjusted R^2_a) for every turbulent flow variables per spatial scale. PCNMs models: XXL: 3–4 m, XL: 2.5–3 m, L: 1.5–2.5 m, M: 1–1.5 m, F: 0.5–1 m, VF: 0.25–0.5 m

DOI: 10.1002/rra

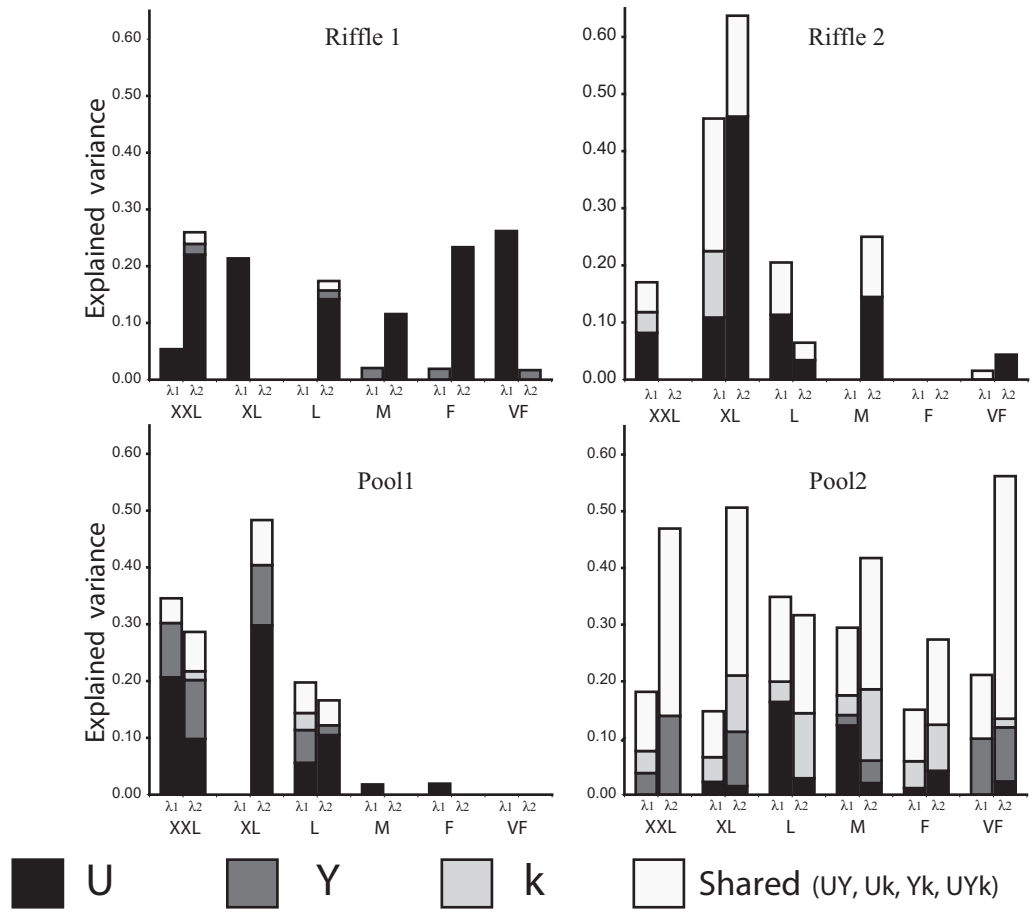

Figure 5. Fraction of variance (R^2_a) of 'scaled turbulence' explained by habitat variables (*Y*: depth (m), *U*: mean streamwise velocity (cm s^{-1}), *k*: bed roughness index (m)). 'Scaled turbulence' represents the first (λ_1) and second (λ_2) canonical axis of each spatial scale (PCNM models)

in Riffle 1, in which the range of habitat values was lower (Table II). The single variable explaining the largest fraction of variation was mean flow velocity, especially in Riffle 1, Riffle 2 and Pool 1. In Pool 2, mean flow velocity also explained a large fraction of turbulent flow properties, but in interaction with flow depth and bed roughness. Flow depth and bed roughness alone did not explain an important fraction of turbulent properties, except for the XXL and XL scales in Pool 1. However, *Y* and *k* had a shared effect in the XL scale in Riffle 2 and in all the range of scales in Pool 2. The fraction of variation explained by multiple variables was very low in Riffle 1 and Pool 1. Generally, in three of the four morphological units, habitat variables explained turbulent flow properties in the larger spatial scales ranging from 1 to 4 m and not much in the finer spatial scales. In Riffle 2 and Pool 1, turbulent flow properties were more strongly affected by *U*, *Y* and *k* at the XL scale. In contrast, turbulent properties in Pool 2 were explained by habitat variables at all scales. However, the first canonical axis (λ_1), which represents the major part of turbulence variability, was better explained by habitat variables at the L and M scales.

DISCUSSION

Spatial scale partitioning of turbulent flow variables

In this study, the extensive high-resolution measurements and a PCNM analysis provided a way to estimate the proportion of turbulent flow variation (R^2_a) associated with six spatial scales ranging from 0.25 to 4.0 m. In the four

DOI: 10.1002/rra

morphological units, turbulent properties exhibited a spatial dependence across the entire range of scales. However, they showed a substantial variability among the units, partly because the units were selected in order to portray the range of hydraulic properties at base flow. In two of the four units, the smaller spatial scales (<1.5 m) explained less variability than the larger scales (>1.5 m). In previous studies that have examined in detail the variability of turbulent flow properties at the reach scale in shallow gravel-bed rivers, Lamarre and Roy (2005) and Legleiter *et al*. (2007) have reported the presence of large spatial patterns of mean turbulent flow properties and the localized effects of individual bed roughness elements on turbulence. The overriding of large scale patterns over the smaller scales could be caused by the presence of large scale coherent turbulent flow structures that are highly energetic and are not much affected by individual roughness elements such a boulders and pebble clusters (Roy *et al*., 2004; Lacey and Roy, 2007). Even though they were larger in size, the reaches presented in previous studies (Lamarre and Roy, 2005; Legleiter *et al*., 2007) were more similar to Riffle 1 and Pool 1 as they were relatively homogenous in terms of the streamwise mean flow velocity (U). These sites do not include patches of high velocity flow with others of very slow flow such as the two more heterogeneous units of this study, Riffle 2 and Pool 2. These two units showed a larger fraction of variance explained by the smaller scales (0.25–1.5 m) than the other units. This scale is typically associated to the turbulent processes such as flow separation and of eddy shedding induced by large roughness elements. The spatial heterogeneity of turbulent flow was previously examined at this scale over a replica of a natural gravel patch ($2\,m^2$) at three heights close to the bed on a $0.05 \times 0.10\,m^2$ systematic sampling grid (Buffin-Belanger *et al*., 2006). At 0.1 m above the bed, the authors observed a relatively low spatial heterogeneity of *RMS* and *TKE*. Furthermore, semi-variance analysis revealed a very low spatial autocorrelation, suggesting that the small variations observed at the patch scale occurred within scales finer than their sampling grid (Buffin-Belanger *et al*., 2006).

In this study, between 30 and 55% of the variability was not explained by PCNM spatial models. A large part of that unexplained variability could be related to the processes occurring at scales smaller than those taken into account by the sampling scheme. At the small scale, turbulent intensities can present very high spatial heterogeneity. For example, at 5 cm above the bed, Stone and Hotchkiss (2007) typically observed variations of as much as 100% over $144\,cm^2$ of bed surface in a riffle, a run and a pool. Similarly, several studies have shown a very high spatial and temporal heterogeneity of turbulent flow at the centimetre scale (Hart *et al*., 1996; Dancey *et al*., 2000). However, flow measurements at this very fine scale were recorded at a few millimetres above the bed. This suggests a high variability of turbulent flow properties at the scales of bed particle size and of river sections, but a relative homogeneity at the intermediate morphological unit/patch scale.

In this study, the choice of sampling velocity at a height of 10 cm was a tradeoff between sampling efficiency and ecological relevance. Even if a significant part of river biota is benthic and rarely leaves the first few centimetres from the bed, turbulent flow properties at 10 cm above the bed are of great importance. For example, fish such as juvenile salmonids spend most of their time sitting and waiting on the river bed and the major part of their swimming energy expenditures is related to burst movements in the water column to catch drifting preys (Hughes and Dill, 1990). Sampling closer to the bed would most likely have resulted in a higher spatial heterogeneity of the flow variables as spatial flow heterogeneity increases with height above the bed. It appears that streamwise velocity becomes spatially homogeneous at a distance varying between two to four times the median bed roughness height (Buffin-Belanger *et al*., 2006).

Our results show that the total portion of variability of turbulent flow explained by the spatial scales was higher in the pools than in the riffles. This could be a consequence of the higher mean flow velocity in riffles than in pools. Previous studies have suggested a decrease of spatial flow heterogeneity associated with an increase of discharge or mean flow velocity, both at the reach scale (Moir *et al*., 2006; Legleiter *et al*., 2007) and at the patch scale (Buffin-Belanger *et al*., 2006). However, the proportion of variation explained by the larger scales (XXL, XL, L) was not higher in the pools. Nevertheless, the spatial organization of near-bed flow may remain similar, as suggested by a strong covariation of hydraulic variables for individual sampling locations at different levels of flow (Buffin-Belanger *et al*., 2006).

The spatial scale partitioning of the variability of 19 individual turbulence variables exhibited a high inter-site variability. However, in general, the mean turbulent flow variables like RMS and TKE displayed a stronger spatial structure than turbulent event variables obtained from quadrant analysis. Q_1 events are often associated to the reattachment point in a separation zone in the lee of obstacles and Q_4 to the frequent low magnitude fast downward

DOI: 10.1002/rra

events induced by the presence of protruding roughness elements (Buffin-Belanger and Roy, 1998). In a recent study, Lacey *et al*. (2007) used the PCNM analysis to quantify the spatial scales of flow variability of a vertical flow field around a pebble cluster ($1.5 \times 0.4\,m^2$). Even at this smaller scale, quadrant-based variables were less spatially structured than the mean turbulent statistics such as RMS. However, in the present study, the great variability between the sites prevented us from making any generalization on the spatial scalings observed between the variables. In Pool 2, most flow variables showed a high similarity of both total R^2_a and the proportions of variation explained by each scale. However, the variability contained in each spatial scale might be differently related to habitat variables.

The link between 'standard' habitat variables and turbulence variables at multiple scales

In the present study, we investigated the relationships between 'standard' fish habitat variables *U*, *Y* and *k* and the variation of turbulent flow variables in four different hydraulic contexts. The explanatory power of 'standard' fish habitat variables at each scale varied greatly between the four morphological units. It was not surprising that mean flow velocity explained the largest proportion of the turbulent flow variation, as the Reynolds number increases linearly with *U*. However, results revealed that correlations were mainly limited to the scales larger than 1.5 m (XXL, L and L). That may be due to the relatively low heterogeneity of *U* in the smaller scales across the reach at a height 0.1 m above the bed, as reported at the patch scale by Buffin-Belanger *et al*. (2006). In contrast, *Y* generally explained low proportions of turbulent flow variation at all scales. This is relatively unexpected, since turbulent coherent flow structures tend to scale with flow depth (Shvidchenko and Pender, 2001; Roy *et al*., 2004; Nikora, 2006). The length of these structures generally ranges from two to six times the flow depth. Thus, an increase in depth could be associated with an augmentation of the magnitude of the variables describing the duration of turbulent structures such as ITS and Q-*d* variables. The weak explanatory power of depth in three of the four morphological units may be partly explained by the relative homogeneity of depth in these units. Indeed, in Pool 2, where the range of depth values was higher, *Y* explained a larger proportion of variation. However, that portion of variation is shared with the effect of *U* and *k* as they are highly intercorrelated. Similarly, the effect of substrate, represented by the bed roughness index, was also relatively low. Numerous studies have previously quantified in detail the spatial distribution of turbulence properties around bed roughness elements (Brayshaw *et al*., 1983; Lawless and Robert, 2001; Lacey and Roy, 2007). Even though pebble clusters and other individual roughness elements cause an increase in turbulent intensity through shedding, this effect is local (Legleiter *et al*., 2007). Although the complex bed configuration is not reflected in the mean turbulent flow properties at the reach scale (Lamarre and Roy, 2005), it was expected that *k* would explain turbulent flow variability at the smallest scales in this study. However, in three of the four units, it was not the case. This is most likely because the footprint of roughness elements was occurring at a scale smaller than the one detected by the VF scale and because the measurements were sampled at 0.1 m above the bed, which represented sometimes as much as 0.25*Y*. Furthermore, in this study, the roughness at a sample site was characterized using the spatial standard deviation of the elevations in a 65 cm square around a measurement point. However, the magnitude of turbulent properties might be inherited from roughness element located further upstream rather than produced by local shear stress, especially at a few centimetres above the bed. Therefore, the roughness upstream from a micro-habitat could also be considered when describing fish habitat.

The difficulty to isolate turbulence properties from standard habitat variables has been pointed out as a main issue in ecohydraulics research (Enders *et al*., 2005; Smith *et al*., 2006). In general, in this study, the standard habitat variables had a relatively low capacity to explain turbulent properties using simple correlations, especially at the smaller scales. That was partly caused by the complex river dynamics system. For instance, within the morphological units, patches of coarse cobble could be found in slow deeper flow presenting low turbulence magnitude as well as in fast shallow flow associated with high turbulence levels. From a practical point of view, this level of complexity suggests that turbulence should be considered as a 'distinct' ecological variable within the range of spatial scales included in this study.

Understanding the linkages between organisms and their hydraulic environment is a critical step in developing predictive models regarding the structure of fluvial ecosystem (Hart and Finelli, 1999). The temporal and spatial scales of flow variability are among the main drivers of numerous fluvial ecological processes (Biggs *et al*., 2005).

DOI: 10.1002/rra

One of the important issues in ecohydraulics research is to identify and match the proper hydraulic scale to the ecological process or organism distribution of interest. As shown in this study, PCNM analysis is an efficient way to identify relevant spatial scales of flow variability. These hydraulic scales could potentially be setting the boundaries of fluvial organisms and territory size or structuring their mobility patterns. For instance, XXL-scale turbulence patterns are affecting drifting invertebrate spatial distribution, as drifting macroinvertebrate concentration is correlated with velocity at the morphological unit scale rather than at the fish micro-habitat scale (Leung *et al*., 2009). In contrast, individual turbulent structures occurring at the M- and VF scales could affect fish feeding movements (Enders *et al*., 2005). Organisms living in more heterogeneous habitats (variability poorly explained by spatial scale variables), such as Riffle 1 and 2 could be less mobile than organisms living in more homogeneous environments, as they could find complementary habitat types (resting, feeding, etc.) closer apart. However, such links between spatial turbulent flow variability and organism behaviour remain to be explored.

Both the spatial scale of turbulent structures and the size of the organisms of interest might be important factors to consider when examining the effect of turbulence on biota (Nikora *et al*., 2003). For instance, bacterial growth is affected by microturbulent flow (Bergstedt *et al*., 2004), the distribution of macroinvertebrates is influenced by coherent structures associated to individual cobbles and boulders (Bouckaert and Davis, 1998) and large scale flow structures can affect the bioenergetics of juvenile fish (Enders *et al*., 2003). Biggs *et al*. (2005) have hypothesized that the scale of the variations would have to be comparable to the organism size (i.e. 0.01–10 times body length) to be felt. The size and magnitude of the acceleration/deceleration in the abrupt boundaries between high and low-speed structures might also play an important role. The size of coherent structures is generally obtained by substituting space for time using time series analysis such as autocorrelation functions, *U-Level* and quadrant analysis. It is still difficult to determine which turbulence statistics are the most relevant to use in different ecological context. Except for the autocorrelation functions, the variables associated to turbulence structures used in this study have not been used in ecohydraulics studies. However, the use of turbulent event detection techniques in future research could possibly reveal new aspects of the effect of flow on organisms. Indeed, results showed that they were generally less spatially structured than the mean turbulent statistics (RMS, TKE) and less correlated with mean flow velocity, which could be an advantage in the context of adding turbulence metrics to physical habitat models. The question of the effect of turbulence on organism habitat use remains to be investigated.

CONCLUSIONS

PCNM analysis was used to partition the variability of turbulent flow properties into spatial scales in four different morphological units of a gravel-bed river. The capability of standard habitat variables to statistically explain turbulent properties was relatively low, especially in the smaller scales. This suggests that future ecohydraulic research should consider turbulence as a distinct variable within the range of scales considered in this study. In the four units, turbulent properties exhibited a spatial dependence across the entire range of scales. In the most homogeneous units, the larger scales explained a greater proportion of the variation than the smaller ones. The results of this study highlight the existence of large-scale turbulent flow patterns. Furthermore, in pools, where the mean streamwise velocity was slower, the overall spatial dependence was higher. PCNM is a useful analytical technique that provides a way to quantify the spatial dependence of individual response variables over a range of spatial scales. By means of spectral decomposition, it presents a great potential for linking organisms spatial distribution to physical habitat at multiple scales in rivers, especially in the context of highly intercorrelated multivariate datasets. Isolating the effect of turbulence on fluvial organisms represents a challenge due to the intercorrelations between the variables that tend to vary with the spatial scale. Further research should attempt to identify the variables and scales that are most relevant to various ecological processes.

ACKNOWLEDGEMENTS

The authors thank the Natural Science and Engineering Council of Canada, the Canadian Foundation for Innovation and the Canada Research Chair program for funding and Julie Thérien, Francis Gagnon, Christine Rozon, Annie Cassista, Simon Roy and Geneviève Marquis for help on the field. Insightful comments from two anonymous referees helped us to improve the paper.

DOI: 10.1002/rra

REFERENCES

Bergstedt MS, Hondzo MM, Cotner JB. 2004. Effects of small scale fluid motion on bacterial growth and respiration. *Freshwater Biology* **49**(1): 28–40.

Best JL. 1993. On the interactions between turbulent flow structure, sediment transport and berdform development: some considerations from recent experimental research. In: Clifford N. J., French J. R. and Hardisty J., Editors. *Turbulence: Perspectives on Flow and Sediment Transport* John Wiley, Chichester, 61–92.

Biggs BJF, Nikora VI, Snelder TH. 2005. Linking scales of flow variability to lotic ecosystem structure and function. *River Research and Applications.* **21**(2–3): 283–298.

Borcard D, Legendre P. 2002. All-scale spatial analysis of ecological data by means of principal coordinates of neighbour matrices. *Ecological Modelling* **153**(1–2): 51–68.

Borcard D, Legendre P, Avois-Jacquet C, Tuomisto H. 2004. Dissecting the spatial structure of ecological data at multiple scales. *Ecology* **85**(7): 1826–1832.

Bouckaert FW, Davis J. 1998. Microflow regimes and the distribution of macroinvertebrates around stream boulders. *Freshwater Biology* **40**(1): 77–86.

Box GEP, Cox DR. 1964. An analysis of transformations. *Journal of Royal Statistical Society Series B* **26**(43): 211–243.

Brayshaw AC, Frostick LE, Reid I. 1983. The hydrodynamics of particle clusters and sediment entrainment in coarse alluvial channels. *Sedimentology* **30**(1): 137–143.

Buffin-Belanger T, Roy AG. 1998. Effects of a pebble cluster on the turbulent structure of a depth-limited flow in a gravel-bed river. *Geomorphology* **25**(3–4): 249–267.

Buffin-Belanger T, Roy AG, Kirkbride AD. 2000. On large-scale flow structures in a gravel-bed river. *Geomorphology* **32**(3–4): 417–435.

Buffin-Belanger T, Roy AG. 2005. 1 min in the life of a river: selecting the optimal record length for the measurement of turbulence in fluvial boundary layers. *Geomorphology* **68**(1–2): 77–94.

Buffin-Belanger T, Rice S, Reid I, Lancaster J. 2006. Spatial heterogeneity of near-bed hydraulics above a patch of river gravel. *Water Resources Research* **42**(4): 12.

Church M. 2006. Multiple scales in rivers, in Habersack H, Piegay H and Rinaldi M (Eds.), Gravel-bed rivers VI: From Process Understanding to River Restoration, Elsevier B. V. pp. 3–32.

Cotel AJ, Webb PW, Tritico H. 2006. Do brown trout choose locations with reduced turbulence? *Transactions of the American Fisheries Society* **135**(3): 610–619.

Dancey CL, Balakrishnan M, Diplas P, Papanicolaou AN. 2000. The spatial inhomogeneity of turbulence above a fully rough, packed bed in open channel flow. *Experiments in Fluids* **29**(4): 402–410.

Dray S, Legendre P, Peres-Neto PR. 2006. Spatial modelling: a comprehensive framework for principal coordinate analysis of neighbour matrices (PCNM). *Ecological Modelling* **196**(3–4): 483–493.

Enders EC, Boisclair D, Roy AG. 2003. The effect of turbulence on the cost of swimming for juvenile atlantic salmon (salmo salar). *Canadian Journal of Fisheries and Aquatic Sciences* **60**(9): 1149–1160.

Enders EC, Buffin-Belanger T, Boisclair D, Roy AG. 2005. The feeding behaviour of juvenile atlantic salmon in relation to turbulent flow. *Journal of Fish Biology* **66**(1): 242–253.

Ezekiel M. 1930. *Methods of correlation analysis*. John Wiley: NJ.

Frechette M, Butman CA, Geyer WR. 1989. The importance of boundary-layer flows in supplying phytoplankton to the benthic suspension feeder Mytilus-edulis-L. *Limnology and Oceanography* **34**(1): 19–36.

Goring DG, Nikora VI. 2002. Despiking acoustic doppler velocimeter data. *Journal of Hydraulic Engineering-Asce* **128**(1): 117–126.

Gower JC. 1966. Some distance properties of latent root and vector methods used in multivariate analysis. *Biometrika* **53**: 325–338.

Hart DD, Clark BD, Jasentuliyana A. 1996. Fine-scale field measurement of benthic flow environments inhabited by stream invertebrates. *Limnology and Oceanography* **41**(2): 297–308.

Hart DD, Finelli CM. 1999. Physical-biological coupling in streams: the pervasive effects of flow on benthic organisms. *Annual Review of Ecology and Systematics* **30**: 363–395.

Hughes NF, Dill LM. 1990. Position choice by drift-feeding salmonids: model and test for Arctic grayling (Thymallus arcticus) in subarctic mountain streams, Interior Alaska. *Canadian Journal of Fisheries and Aquatic Sciences* **47**: 2039–2048.

Labiod C, Godillot R, Caussade B. 2007. The relationship between stream periphyton dynamics and near-bed turbulence in rough open-channel flow. *Ecological Modelling* **209**(2–4): 78–96.

Lacey RWJ, Legendre P, Roy AG. 2007. Spatial-scale partitioning of in situ turbulent flow data over a pebble cluster in a gravel-bed river. *Water Resources Research* **43**: 3.

Lacey RWJ, Roy AG. 2007. A comparative study of the turbulent flow field with and without a pebble cluster in a gravel bed river. *Water Resources Research* **43**(5): 7.

Lamarre H, Roy AG. 2005. Reach scale variability of turbulent flow characteristics in a gravel-bed river. *Geomorphology* **68**(1–2): 95–113.

Lamarre H. 2006. Sediment transport, sedimentary structures and bed stability in step-pool channels. PhD thesis. Université de Montréal, 293 p.

Lane SN, Biron PM, Bradbrook KF, Butler JB, Chandler JH, Crowell MD, Mclelland SJ, Richards KS, Roy AG. 1998. Three-dimensional measurement of river channel flow processes using acoustic doppler velocimetry. *Earth Surface Processes and Landforms* **23**(13): 1247–1267.

Lawless M, Robert A. 2001. Three-dimensional flow structure around small-scale bedforms in a simulated gravel-bed environment. *Earth Surface Processes and Landforms* **26**(5): 507–522.

Legendre P. 1993. Spatial autocorrelation: trouble or new paradigm? *Ecology* **74**: 1659–1673.

DOI: 10.1002/rra

Legendre P, Legendre L. 1998. *Numerical Ecology. Developments in Environmental Modelling 20*. Elsevier: Amsterdam.
Legleiter CJ, Phelps TL, Wohl EE. 2007. Geostatistical analysis of the effects of stage and roughness on reach-scale spatial patterns of velocity and turbulence intensity. *Geomorphology* **83**(3–4): 322–345.
Leung ES, Rosenfeld JS, Bernhardt JR. 2009. Habitat effects on invertebrate drift in a small trout stream: implications for prey availability to drift-feeding fish. *Hydrobiologia* **623**(1): 113–125.
Liao JC, Beal DN, Lauder GV, Triantafyllou MS. 2003. Fish exploiting vortices decrease muscle activity. *Science* **302**(5650): 1566–1569.
Liao JC. 2007. A review of fish swimming mechanics and behaviour in altered flows. *Philosophical Transactions of the Royal Society B-Biological Sciences* **362**(1487): 1973–1993.
Liu Z, Adrian RJ, Hanratty TJ. 2001. Large-scale modes of turbulent channel flow: transport and structure. *Journal of Fluid Mechanics* **448**: 53–80.
Lu S, Willmarth W. 1973. Measurement of the structure of the Reynolds stress in a turbulent boundary layer. *Journal of Fluid Mechanics* **60**: 472–478.
Luchik TS, Tiederman WG. 1987. Timescale and structure of ejections and bursts in turbulent channel flows. *Journal of Fluid Mechanics* **174**: 529–552.
Moir HJ, Gibbins CN, Soulsby C, Webb JH. 2006. Discharge and hydraulic interactions in contrasting channel morphologies and their influence on site utilization by spawning Atlantic salmon (Salmo salar). *Canadian Journal of Fisheries and Aquatic Sciences* **63**(11): 2567–2585.
Moir HJ, Pasternack GB. 2008. Relationships between mesoscale morphological units, stream hydraulics and Chinook salmon (Oncorhynchus tshawytscha) spawning habitat on the Lower Yuba River, California. *Geomorphology* **100**(3–4): 527–548.
Nikora VI, Goring DG, Biggs BJF. 1998. On gravel-bed roughness characterization. *Water Resources Research* **34**(3): 517–527.
Nikora VI, Aberle J, Biggs BJF, Jowett IG, Sykes JRE. 2003. Effects of fish size, time-to-fatigue and turbulence on swimming performance: a case study of Galaxias maculatus. *Journal of Fish Biology* **63**(6): 1365–1382.
Nikora V. 2006. Hydrodynamics of gravel-bed rivers, scale issues, in Habersack H, Piegay H and Rinaldi M (Eds), Gravel-bed rivers VI: From Process Understanding to River Restoration, Elsevier B. V. pp. 61–84.
Oksanen J, Kindt R, Legendre P, O'Hara RB. 2007. *Community Ecology Package version 1.8–6*. http://cran.r-project.org/
Quinn JM, Hickey CW, Linklater W. 1996. Hydraulic influences on periphyton and benthic macroinvertebrates: Simulating the effects of upstream bed roughness. *Freshwater Biology* **35**(2): 301–309.
Roy AG, Buffin-Belanger T, Lamarre H, Kirkbride AD. 2004. Size, shape and dynamics of large-scale turbulent flow structures in a gravel-bed river. *Journal of Fluid Mechanics* **500**: 1–27.
Shvidchenko AB, Pender G. 2001. Macroturbulent structure of open-channel flow over gravel beds. *Water Resources Research* **37**(3): 709–719.
Smith DL, Brannon EL, Odeh M. 2005. Response of juvenile rainbow trout to turbulence produced by prismatoidal shapes. *Transactions of the American Fisheries Society* **134**(3): 741–753.
Smith DL, Brannon EL, Shafii B, Odeh M. 2006. Use of the average and fluctuating velocity components for estimation of volitional rainbow trout density. *Transactions of the American Fisheries Society* **135**(2): 431–441.
Smith DL, Brannon EL. 2007. Influence of cover on mean column hydraulic characteristics in small pool riffle morphology streams. *River Research and Applications* **23**(2): 125–139.
Stoecker DK, Long A, Suttles SE, Sanford LP. 2006. Effect of small-scale shear on grazing and growth of the dinoflagellate Pfiesteria piscicida. *Harmful Algae* **5**: 407–418.
Stone MC, Hotchkiss RH. 2007. Turbulence descriptions in two cobble-bed river reaches. *Journal of Hydraulic Engineering-Asce* **133**(12): 1367–1378.
Tritico HM, Hotchkiss RH. 2005. Unobstructed and obstructed turbulent flow in gravel bed rivers. *Journal of Hydraulic Engineering-Asce* **131**(8): 635–645.
Weissburg MJ, Zimmerfaust RK. 1993. Life and death in moving fluids—hydrodynamic effects on chemosensory-mediated predation. *Ecology* **74**(5): 1428–1443.
Wolman MG. 1954. A method of sampling coarse river-bed material. *Transactions of the American Geophysical Union* **35**(6): 951–956.

DOI: 10.1002/rra